Journal of Intelligent and Connected Vehicles
2024, 7(1): 19–29
https://doi.org/10.26599/JICV.2023.9210025

Research Article

Intelligent decision-making method for vehicles in emergency conditions based on artificial potential fields and finite state machines

Xunjia Zheng[1,2], Huilan Li[3], Qiang Zhang[1], Yonggang Liu[4], Xing Chen[2], Hui Liu[2], Tianhong Luo[2], Jianjie Gao[5,✉], Lihong Xia[1]

[1]*China Automotive Engineering Research Institute Co., Ltd., Chongqing 401122, China*
[2]*School of Intelligent Manufacturing Engineering, Chongqing University of Arts and Sciences, Chongqing 402160, China*
[3]*Department of Information and Intelligence Engineering, Chongqing City Vocational College, Chongqing 402160, China*
[4]*College of Mechanical and Vehicle Engineering, Chongqing University, Chongqing 400044, China*
[5]*Intelligent Policing Key Laboratory of Sichuan Province, Luzhou 646000, China*

Received: September 24, 2023; Revised: October 18, 2023; Accepted: November 6, 2023

ABSTRACT: This study aims to propose a decision-making method based on artificial potential fields (APFs) and finite state machines (FSMs) in emergency conditions. This study presents a decision-making method based on APFs and FSMs for emergency conditions. By modeling the longitudinal and lateral potential energy fields of the vehicle, the driving state is identified, and the trigger conditions are provided for path planning during lane changing. In addition, this study also designed the state transition rules based on the longitudinal and lateral virtual forces. It established the vehicle decision-making model based on the finite state machine to ensure driving safety in emergency situations. To illustrate the performance of the decision-making model by considering APFs and finite state machines. The version of the model in the co-simulation platform of MATLAB and CarSim shows that the developed decision model in this study accurately generates driving behaviors of the vehicle at different time intervals. The contributions of this study are two-fold. A hierarchical vehicle state machine decision model is proposed to enhance driving safety in emergency scenarios. Mathematical models for determining the transition thresholds of lateral and longitudinal vehicle states are established based on the vehicle potential field model, leading to the formulation of transition rules between different states of autonomous vehicles (AVs).

KEYWORDS: decision-making, artificial potential field, finite state machines, emergency conditions, autonomous driving

1 Introduction

Considering the rapid advancements in autonomous vehicles (AVs) and transportation technology, ensuring the safety and reliability of vehicles in emergency conditions is crucial (Guo et al., 2022; Liu et al., 2023a; Wang et al., 2022b). From unexpected obstacles on the road to sudden weather changes and unforeseen traffic incidents, vehicles operating in real-world environments must possess the capability to make intelligent decisions swiftly and effectively to avoid accidents and ensure the safety of passengers and pedestrians alike (He et al., 2023; Liang et al., 2021; Liu et al., 2021).

For autonomous driving, the critical challenge of ensuring safe and efficient decision-making in emergencies persists. One promising approach to tackle this challenge is the integration of artificial potential fields (APFs) and finite state machines (FSMs) (Liu et al., 2023b; Palatti et al., 2021). This amalgamation harnesses the strengths of both methodologies, providing a robust framework for intelligent decision-making under high-stress conditions. APFs, originally developed for robotics and path planning, have been adapted for autonomous vehicle control (Li et al., 2022; Ma et al., 2023a, 2023b; Xie et al., 2022; Zheng et al., 2018). These fields create virtual forces that guide the vehicle away from obstacles or toward a desired destination (Rasekhipour et al., 2017). During emergencies, such as unexpected obstacles in the road, APFs can rapidly calculate and apply corrective forces to avoid collisions, a vital feature for ensuring passenger safety (Nguyen et al., 2023). Finite state machines (FSMs), offer a structured methodology to represent and manage complex decision-making processes (Wang et al., 2022a). FSMs break down decision-making into discrete states and transitions, allowing vehicles to switch between predefined behaviors based on sensor inputs and system conditions (Wang et al., 2021). In emergency scenarios, FSMs enable swift transitions to appropriate response modes, such as emergency braking or evasive maneuvers (Jaswanth et al., 2022).

This study introduces an innovative method that combines the principles of APFs and FSMs to enhance the decision-making capabilities of vehicles in emergency situations. By simulating the concept of potential fields, the method enhances a vehicle's capacity for environmental perception and hazard assessment, consequently facilitating navigation through complex scenarios with elevated safety and precision. Coupled with FSMs, which provide a structured framework for decision-making, this approach empowers vehicles to choose the most appropriate

✉ Corresponding author.
E-mail: jianjiecq@163.com

actions in response to a wide range of emergency situations.

In the following sections, we will delve deeper into the theoretical underpinnings of APFs and FSMs, exploring their individual strengths and how their synergy can revolutionize vehicle decision-making in emergencies. We will also discuss the practical implications of implementing this intelligent decision-making method, including its potential to reduce accidents, improve traffic flow, and pave the way for more dependable autonomous transportation systems. The fusion of APFs and FSMs represents a significant step towards enhancing the safety and reliability of vehicles during emergency conditions, ushering in a new era of intelligent transportation systems capable of navigating the most challenging scenarios with precision and effectiveness. The main contributions include:

1) Analysis of driving behavior in emergency conditions: This study defines scenarios involving emergency conditions by analyzing and categorizing vehicle driving conditions. It examines the influencing factors affecting decision-making processes during emergencies and establishes a decision-making framework for AVs operating in emergencies.

2) Virtual potential field-based modeling of vehicle behavior: Addressing the challenge of dynamically determining threshold values for longitudinal state transitions in vehicles, the study proposes a longitudinal graded safety potential field force model based on vehicle longitudinal motion dynamics.

3) State machine decision methods based on artificial potential field forces: This study formulates a vehicle state machine decision model predicated on the foundational principles of FSMs. It formulates transition rules for different vehicle driving states and develops a layered decision state machine model in Simulink/Stateflow.

The rest of this paper is organized as follows. In Section 2, we analyze the driver behavior under emergency conditions. Section 3 establishes an artificial potential field model for calculating the driving risk. Section 4 establishes a decision-making model considering artificial potential field and FSMs. Section 5 conducts joint simulation verification using Matlab and Carsim. Section 6 concludes the study.

2 Analysis of driver behavior under emergency conditions

2.1 Selection of emergency driving scenarios

Based on the crash accident data from the Crash Report Sampling System (CRSS) of the U.S. Department of Transportation's National Highway Traffic Safety Administration (NHTSA), it emerges that motor vehicles significantly lead in the proportion of traffic accidents involving casualties. Among these accidents, the largest share is attributed to accidents caused by improper driver behavior, accounting for approximately 83% of the total accidents. Improper driver behaviors mainly include emergency braking, lane-changing without caution, driving in the wrong direction, and stopping on the roadway due to vehicle malfunction. Specifically, accidents caused by vehicle braking account for 10.9% of the total, lane-changing accidents account for 11.8%, wrong-way driving accounts for 3.1%, and accidents resulting from stopping on the roadway constitute 0.3%.

It is evident that emergency braking, lane-changing, and vehicle malfunctions contribute significantly to driver behavior-related accidents. As this investigation does not consider illegal driving behaviors, the aspect of wrong-way driving is excluded from the research, and the focus is placed on the remaining three driving conditions for analysis.

2.2 Driver behavior analysis

Based on the distinct vehicle operational zones, driving behaviors under emergency conditions are categorized into free driving, car-following, emergency braking, and emergency lane changing, as illustrated in Fig. 1.

1) Free driving. Free driving represents the optimal state of a vehicle operating on the road, where the vehicle maintains the desired speed and an adequate safe following distance according to the driver's intent before encountering emergency scenarios. Lane changes are also permissible during this state.

2) Car-following. Vehicle following occurs when the subject vehicle adjusts its speed, following a preceding vehicle that undergoes braking and subsequent acceleration. In this scenario, the primary vehicle aims to ensure driving safety by modulating throttle opening and braking force to adapt the follower vehicle's speed.

3) Emergency braking. During car-following scenarios, when the subject vehicle encounters sudden braking by the lead vehicle or the abrupt appearance of an obstructing vehicle ahead, and the ambient environmental conditions do not satisfy the requirements for a lane-change evasion, the intelligent vehicle applies significant braking force to avert collision with the obstructing vehicle.

4) Emergency lane changing. Emergency lane change occurs when the vehicle's safety requirements cannot be met solely by emergency braking. In this scenario, the driver modifies the vehicle's trajectory by steering to avoid collision with obstructing vehicles. This maneuver encompasses two forms: braking-induced lane change and acceleration-induced lane change.

2.3 Analysis of factors influencing emergency decision-making

The driving behavior decision mechanism is vital to road traffic system safety. Sound and timely decision-making form the foundation of establishing such mechanisms; hence, analyzing the factors influencing decision-making is significant. Distinct

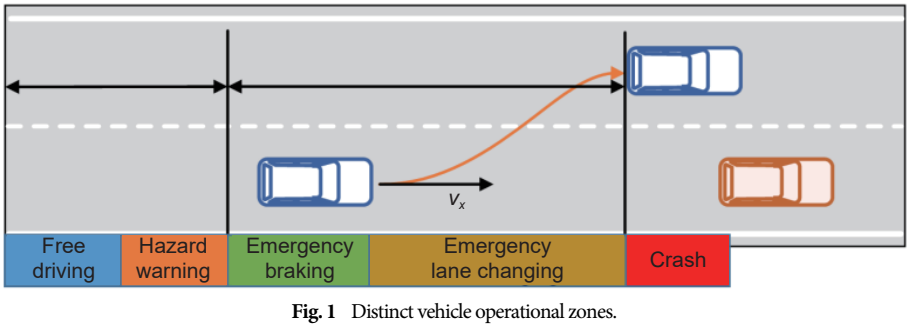

Fig. 1 Distinct vehicle operational zones.

decision mechanisms arise from varying vehicle types, velocities, and road driving conditions. While the complexity and dynamism inherent in the road traffic domain pose significant challenges for a comprehensive analysis of decision-making mechanisms across a multitude of driving scenarios. To address this issue, the establishment of representative scenario models becomes imperative. As delineated in Section 2.2, which focused on emergency scenarios, collision severity served as the critical metric for identifying the research scenario of interest. This study employs collision severity as a metric to analyze the principal factors impacting driving decisions.

2.3.1 *Vehicle type*

Vehicles, as the central entities within the transportation system, represent the primary subjects contributing to accidents. Collision factors related to vehicles predominantly encompass vehicle attributes and safety configurations. Vehicle details contain vehicle type, powertrain characteristics, and stability. Safety configurations surround lighting, braking systems, and other vehicle safety features. Among these factors, varying vehicle types result in substantial disparities in vehicle weight. Under otherwise similar conditions, greater mass imparts higher inertia, leading to significant braking effectiveness differences during emergencies. Consequently, the requisite safe following distance or collision reaction time varies considerably.

Fig. 2 describes the distribution of different vehicle types involved in traffic accidents within the NASS/GES dataset. Statistical data analysis reveals that passenger cars and light trucks contribute the highest proportion to accident occurrences. Within the category of passenger cars, the balance of severe accidents is similar to that of light trucks. However, for moderate and minor accidents, the proportion of passenger cars surpasses that of light trucks. Compact vehicles exhibit a significantly higher likelihood of accident occurrence and severity in road traffic accidents than other vehicle types.

2.3.2 *Vehicle velocity*

Vehicle velocity is a crucial performance metric within the vehicle decision-making system, and accidents resulting from excessive speeds are notably common in traffic incidents. Elevated vehicle speed leads to an increase in both driver reaction distance and vehicle braking distance. Moreover, excessive speed can reduce the contact force between the tires and the road surface for vehicles with lighter payloads, potentially resulting in instability when steering. On road segments with minimum speed limits, excessively low speeds can lead to traffic congestion and a heightened risk of rear-end collisions. Therefore, the selection of appropriate vehicle speeds during travel is of paramount importance in terms of optimizing road traffic efficiency.

Fig. 3 illustrates the proportion of accidents occurring in different vehicle speed intervals. It can be observed from the graph that as the vehicle speed increases, the proportion of severe collision incidents between vehicles gradually escalates. In cases of moderate and minor collision incidents, higher proportions are

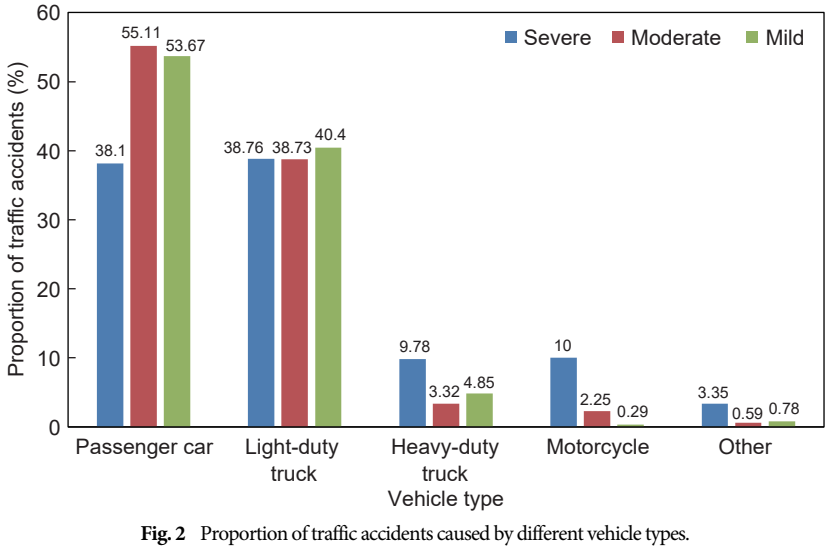

Fig. 2 Proportion of traffic accidents caused by different vehicle types.

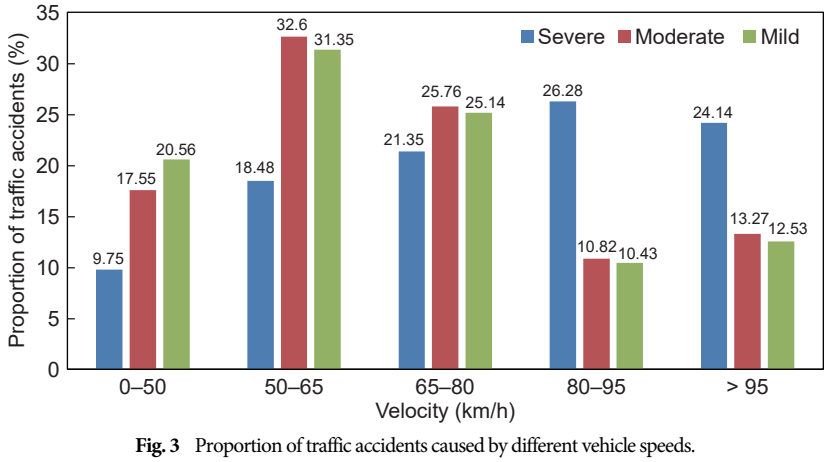

Fig. 3 Proportion of traffic accidents caused by different vehicle speeds.

evident within the context of moderate to low speeds.

2.3.3 *Road type*

Road transportation serves as the conduit for vehicle operations, where vehicles formulate driving decisions based on diverse road conditions. Dynamic decision-making is employed to ensure safe vehicle operations on varying road surfaces. Rational road design, appropriate selection of road materials, and timely road maintenance constitute fundamental requisites for providing safe travel. Specifically, the sound design of road structures encompasses aspects such as road alignment and pavement conditions.

The linear structure of a road encompasses its curvature and gradient, influencing vehicle obstacle avoidance decisions. Fig. 4 presents statistical data regarding road linear structure types from the NASS/DES dataset. Based on curvature, the dataset categorizes roads into straight and curved segments, while based on gradient, roads are classified into level and inclined segments. Notably, the data reveals that level roads are associated with a higher rate of accidents compared to inclined roads. Moreover, accidents involving straight-line vehicle travel on level roads exhibit a higher rate compared to curved-road scenarios.

By analyzing the impact of vehicle attributes, velocity, and road types on the severity of vehicle collisions, scenario-based modeling is established for vehicles, simulated road conditions, and velocities under emergency conditions.

2.4 Framework for emergency decision-making process

The installation of advanced environmental perception and self-state detection devices is imperative to facilitate the safe operation of AVs within complex road environments. These devices continuously monitor dynamic information concerning surrounding vehicles during the driving process. Under emergency conditions, AVs require decision commands to transition between various driving states. Consequently, formulating transition rules between these states serves as a prerequisite to ensuring accurate command outputs.

Fig. 5 illustrates the flowchart of emergency decision-making for AVs under emergency conditions. When an autonomous vehicle encounters an emergency, the data collected by the vehicle's perception system undergoes filtering, processing, and fusion. This data refinement leads to the determination of the type of emergency scenario. Subsequently, a potential field force model between the two vehicles is established using the data information. This model then compares with dynamic thresholds and formulated state transition rules specific to the scenario. This analysis aids in predicting the upcoming vehicle state, which facilitates the generation of driving decision commands for transmission to the vehicle's control execution system. Upon receiving these decision commands, the autonomous vehicle engages its control actuators, determining the magnitude of braking torque and steering wheel angle based on an analysis of the vehicle's kinematics and dynamics.

3 Artificial potential field virtual force modeling

According to the theory of artificial potential fields, other road users around the vehicle and road boundaries (such as lane

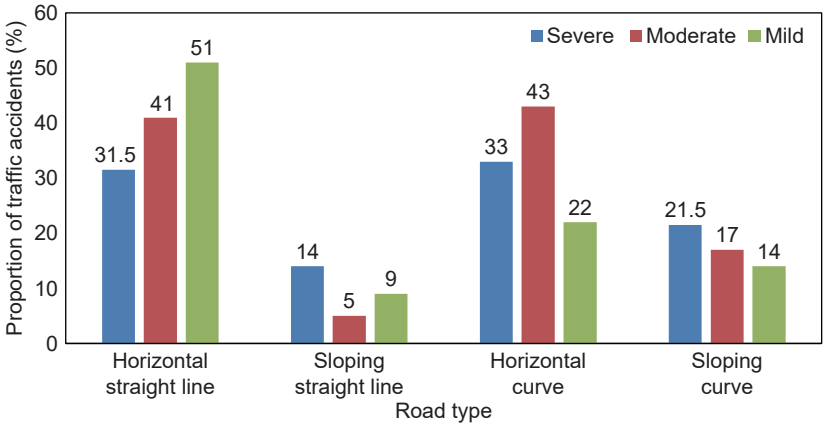

Fig. 4 Proportion of traffic accidents caused by different road types.

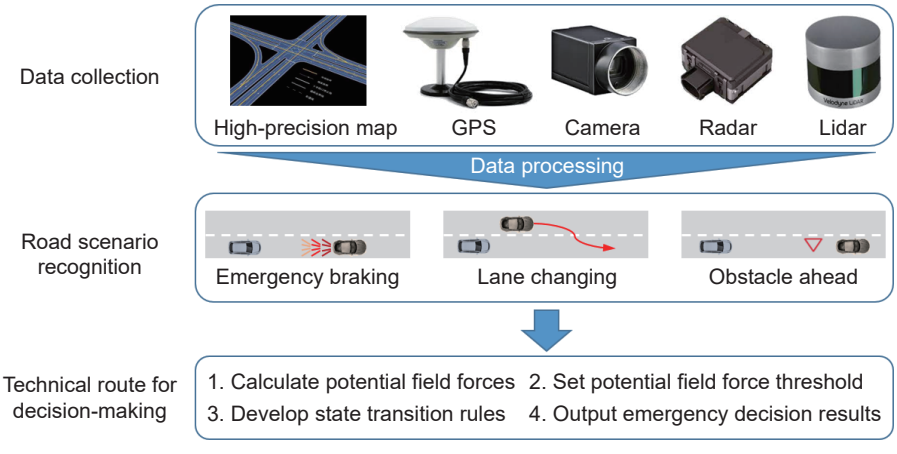

Fig. 5 Flowchart of emergency decision-making process.

markings) generate repulsive forces, while the destination exerts an attractive force on the vehicle. Considering the combined effect of virtual forces in various directions, the vehicle moves along the intended trajectory, ensuring safe travel. To facilitate the analysis of the forces acting on the vehicle and to accurately plan the vehicle's trajectory, this study models the potential field forces separately in the longitudinal and lateral directions, as shown in Eq. (1):

$$\begin{cases} F_X = F_{ax} + F_{px} \\ F_Y = F_{ay} + F_{py} + F_b + F_l \end{cases} \tag{1}$$

where F_X represents the longitudinal virtual potential field force, F_Y denotes the lateral virtual potential field force. F_{ax} and F_{ay} stand for the virtual attractive forces exerted on the target vehicle in the longitudinal and lateral directions, respectively. F_{px} and F_{py} correspond to the virtual repulsive forces acting on the target vehicle in the longitudinal and lateral directions, respectively. F_b and F_l represent the repulsive forces generated by road boundaries and lane markings, respectively.

3.1 Longitudinal virtual potential field force

3.1.1 Longitudinal repulsive force

According to the theory of artificial potential fields, the expression for the potential field force generated by vehicle i is defined as shown in Eq. (2):

$$F_i = k_i m_i \frac{v_i^2}{d^n} \tag{2}$$

where F_i represents the field force exerted by vehicle i on the external environment, k_i is the vehicle kinetic energy coefficient ($0 < k_i \leq 1$), m_i stands for the mass of vehicle i, v_i denotes the velocity of vehicle i, d is the distance from the center of mass of vehicle i to a certain point in the vicinity, and n represents the position gradient index.

Simultaneously, considering that the field force does not grow infinitely, within a small distance $d_{\min}$, the risk value remains constant, expressed as

$$F_{i,\max} = k_i m_i \frac{v_i^2}{d_{\min}^n} \tag{3}$$

Based on this property, the modeling of longitudinal repulsive force is established as

$$F_i = \begin{cases} F_{i,\max} & d < d_{\min} \\ k_i m_i \dfrac{v_i^2}{d^n} & d_{\min} \leq d \leq d_{\max} \\ 0 & d > d_{\max} \end{cases} \tag{4}$$

where $d_{\min}$ represents the distance at which the potential field force reaches its maximum value, $d_{\max}$ signifies the distance at which the potential field force exerts its maximum effect, and $F_{i,\max}$ denotes the maximum virtual potential field force exerted on the vehicle.

The normalization and standardization are required to obtain a standardized mathematical model for potential field force, given the presence of both significant maximum and minimum values in the potential field force. Therefore, the normalization processing is conducted by Eq. (5):

$$F_g = \frac{F_i - F_{i,\min}}{F_{i,\max} - F_{i,\min}} \tag{5}$$

The resultant normalized mathematical model for potential field force is presented as Eq. (6):

$$F_p = \begin{cases} 1 & d < d_{\min} \\ \dfrac{d^{-n} - d_{\max}^{-n}}{d_{\min}^{-n} - d_{\max}^{-n}} & d_{\min} \leq d \leq d_{\max} \\ 0 & d > d_{\max} \end{cases} \tag{6}$$

After transforming the longitudinal repulsive force into the road coordinate system, the resulting final repulsive potential field force model is presented as Eq. (7):

$$F_p = \begin{cases} 1 & d < d_{\min} \\ \dfrac{\left[(x-x_0)^2 + (y-y_0)^2\right]^{-n} - d_{\max}^{-n}}{d_{\min}^{-n} - d_{\max}^{-n}} & d_{\min} \leq d \leq d_{\max} \\ 0 & d > d_{\max} \end{cases} \tag{7}$$

where (x, y) represents the position coordinates of the target vehicle, and (x_0, y_0) represents the position coordinates of the obstacle.

3.1.2 Longitudinal attractive force

The longitudinal attractive force experienced by the target vehicle exhibits similar characteristics to that of the repulsive force. That is, the farther the vehicle is from the destination, the smaller the magnitude of the longitudinal attractive force it experiences, and conversely, the closer it is to the destination, the greater the magnitude of the longitudinal attractive force. During the driving process, the target vehicle always aims to maintain a certain safe following distance to ensure safe travel. When the vehicle spacing satisfies this safe distance and is additionally influenced by the attractive force toward the destination, the target vehicle accelerates or overtakes. Similar to the modeling approach for longitudinal repulsive force, the longitudinal attractive force model is defined as presented in Eq. (8):

$$F_a = \begin{cases} 1 & x > x_{\max} \\ \dfrac{x^{-m} - x_{\min}^{-m}}{x_{\max}^{-m} - x_{\min}^{-m}} & x_{\min} \leq x \leq x_{\max} \\ 0 & x < x_{\min} \end{cases} \tag{8}$$

where F_a represents the longitudinal attractive force; m denotes the force coefficient; $x_{\min}$ and $x_{\max}$ represent the distance to the lead vehicle when the attractive force is at its minimum and maximum value, respectively. x denotes the distance from the vehicle's target point to the vehicle.

3.2 Lateral virtual potential field force

3.2.1 Lateral repulsive force

The road boundary line defines the lateral edge of the road, determining the lateral permissible range of vehicle movement. Lane markings constrain vehicles to adhere to regulated travel on the street, enhancing road safety. Unlike road boundary lines, lane markings hold vehicle movement while allowing vehicles to cross lane boundaries for lane-changing and overtaking maneuvers. Typically, vehicles travel along the roads' centerline. During this movement, vehicles experience minimal constraint from lane markings and road boundaries, with the constraint force being highest when nearing the lane markings.

To represent the force characteristics experienced by vehicles within the road potential field, a potential field force of one is designated at the road boundary line position. In contrast, a

potential field force of zero is assigned at the centerline position of each lane. By utilizing trigonometric functions, the lateral potential field force model for vehicles is established as presented in Eq. (9):

$$F_h = A\left(\cos\frac{2\pi y}{D_b}+1\right) \tag{9}$$

where F_h represents the lateral potential field force caused by road boundary line, A represents the magnitude of the potential field force function, y denotes the lateral position coordinate of the vehicle, and D_b stands for the width of the lane marking. The relationship between the magnitude of the potential field force function and the lateral coordinate along the lane centerline is expressed as shown in Eq. (10):

$$A = \frac{1-\lambda}{4n-4}\left(|\mathrm{sgn}\,(y-x_1)| + \sum\nolimits_{n=2}^{u}|\mathrm{sgn}\,(y-x_n)|\right)+\lambda/4 \tag{10}$$

where λ represents the lateral potential field force coefficient, and u signifies the number of lanes in the same direction. x_n corresponds to the longitudinal coordinate of the center of the n-th lane marking.

3.2.2 *Lateral repulsive force*

The driver's intention to change lanes or overtake can be considered the vehicle's proactive alteration of its current driving state under the influence of the target lane's attraction. Setting the position of the lane's centerline in the target lane as the point of attraction, a lateral attraction model can be established as presented in Eq. (11):

$$F_c = \begin{bmatrix} k_l & 0 \\ 0 & k_r \end{bmatrix}\begin{bmatrix} (y-y_0)^a/\Delta y \\ -(y-y_0)^a/\Delta y \end{bmatrix} \tag{11}$$

where F_c represents the lateral attractive force on the vehicle; k_l and k_r denote the lateral decision coefficients represented by the left and right lane lines, respectively. y represents the longitudinal position coordinate of the target vehicle, y_0 signifies the longitudinal coordinate of the centerline of the current target vehicle's lane, a means the longitudinal position gradient index, and Δy stands for the width of the lane.

The construction of the lateral attraction model primarily involves identifying the vehicle's operational state. When exploring the lateral decision coefficients of vehicles, it is essential to consider the velocity and positional information of both the target vehicle and the surrounding vehicles. Accurately identifying the lateral driving intention of the vehicle ensures safety during lane changing and overtaking while also providing triggering conditions for trajectory planning during lane changes. As a result, this study will conduct an in-depth analysis of the determination of lateral decision coefficients in Section 4.

4 Decision-making model considering APF and FSM

The process of vehicle movement on the road can be regarded as the switching of different vehicle states at various moments, and state machines are commonly used methods to describe the process of vehicle state transitions. However, the time-varying and complex road traffic environment makes it challenging to determine state transition conditions accurately. This study proposes a longitudinal hierarchical safety potential field model based on vehicle kinematics to address the difficulty in precisely defining state thresholds during dynamic vehicle movement.

The vehicle driving states are divided into three categories: free driving, car-following, and emergency braking. Correspondingly, the longitudinal movement is divided into three levels. The hierarchy of states is presented in Table 1, which provides an overview of different vehicle driving states corresponding to each level.

Table 1 Hierarchical level

Level	Driving state
1	Free driving
2	Car-following
3	Emergency braking

A vehicle's driving behavior while driving straight is primarily influenced by the actions of the vehicles in front. Assuming that the vehicle brakes with maximum deceleration until it comes to a complete stop and neglecting other resistances during the driving process, let D_1 and D_2 be the thresholds for the following distance of level 2 and the emergency braking distance of level 3, respectively. This can be derived as Eqs. (12) and (13):

$$D_1 = \frac{v_i^2}{a_{\max 1}} + k_t v_i - \frac{v_j^2}{2a_{\max 2}} \tag{12}$$

$$D_2 = \frac{v_i^2}{2a_{\max 1}} + k_t v_i - \frac{v_j^2}{2a_{\max 2}} \tag{13}$$

where $a_{\max 1}$ and $a_{\max 2}$ denote the maximum deceleration of vehicles i and j, respectively; and k represents the ratio between the safe following distance and the vehicle's speed. In other words, k is the time headway (THW), and we take a value of 1.5 s.

By combining Eqs. (12) and (13) with Eq. (6), the thresholds for longitudinal potential forces of different levels can be obtained:

$$F_G = k_t\frac{D_2^{-n} - d_{\max}^{-n}}{d_{\min}^{-n} - d_{\max}^{-n}} \tag{14}$$

$$F_B = k_t\frac{D_1^{-n} - d_{\max}^{-n}}{d_{\min}^{-n} - d_{\max}^{-n}} \tag{15}$$

where F_G represents the potential force threshold for the following state, and F_B is the potential force threshold for the emergency braking state. It can be observed that the potential force thresholds for different states are continually changing based on the variations in target and leading vehicle speeds.

Hierarchical finite state machine (HFSM), an extension of FSM, is also known as a layered state machine. It comprises multiple finite-state machines and is employed for complex decision-making systems due to its logical coherence, clear structure, and enhanced processing efficiency.

Fig. 6 depicts establishing the decision model in this study, where vehicle state transition rules are designed. The decision-making process for the vehicle is divided into longitudinal and lateral processes using a hierarchical state machine. Simulink/Stateflow is utilized to create both longitudinal and lateral decision models. Finally, the vehicle's driving behavior decision model is constructed using MATLAB/Simulink.

4.1 Formulation of state transition rules

The preceding analysis encompassed the four driving behaviors of AVs under emergency conditions: free driving, car-following, emergency braking, and emergency lane change. These behaviors are established as the state set for the state machine model,

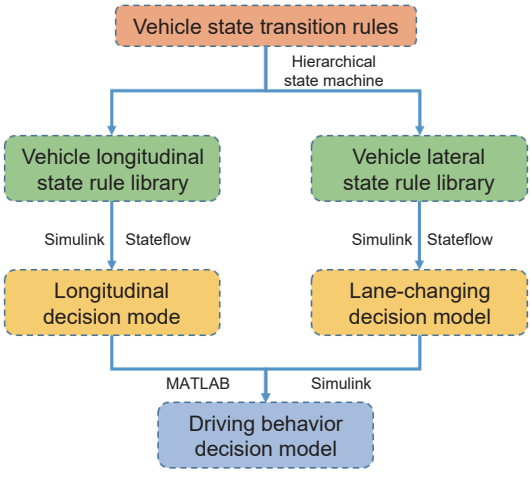

Fig. 6 Decision-making model modeling process.

wherein the longitudinal state set consists of free driving, following mode, and emergency braking. While the lateral state set comprises emergency lane change. Utilizing the developed vehicle virtual potential field forces to explore dynamic thresholds across different scenarios and incorporating surrounding vehicle speeds as conditions for state transitions, the initial state of the vehicle state machine is set to free driving.

To facilitate the representation of vehicle states and the output of results, the attributes of states are defined according to Table 2. Specifically, state 0 signifies free driving, state 1 represents following mode, state 2 corresponds to emergency braking, and state 3 indicates emergency lane change.

Table 2 State attribute value information

State attribute value	Meaning of state attribute values
0	Free-driving
1	Car-following
2	Emergency braking
3	Emergency lane-changing

4.2 Formulation of longitudinal state transition rules

The state transition of AVs is based on the resultant force between the ego vehicle and the preceding vehicle while driving straight, as expressed in Eq. (16):

$$F_{ap} = F_p + F_a \tag{16}$$

By combining Eqs. (12), (13), and (16), the threshold values for potential field forces in the following mode and emergency braking mode are obtained, as shown in Eqs. (17) and (18), respectively:

$$F_{cf} = k_p \frac{D_1^{-n} - d_{\max}^{-n}}{d_{\min}^{-n} - d_{\max}^{-n}} + k_a \frac{D_1^{-n} - x_{\min}^{-n}}{x_{\max}^{-n} - d_{\min}^{-n}} \tag{17}$$

$$F_{eb} = k_p \frac{D_2^{-n} - d_{\max}^{-n}}{d_{\min}^{-n} - d_{\max}^{-n}} + k_a \frac{D_2^{-n} - x_{\min}^{-n}}{x_{\max}^{-n} - x_{\min}^{-n}} \tag{18}$$

After establishing the vehicle's potential field force model and obtaining information about surrounding vehicles, the longitudinal decision transition rules for AVs can be analyzed as follows.

In emergencies, if the resultant potential field force between the target vehicle and the preceding vehicle in the same lane is less than the vehicle's following potential field force threshold ($F_{ap} < F_{cf}$), the lateral decision coefficient is set to 0, and the target vehicle maintains the free-driving state. If the resultant potential field force between the target vehicle and the preceding vehicle falls within the range between the vehicle's following and emergency braking thresholds ($F_{cf} \le F_{ap} \le F_{eb}$), with the preceding vehicle's speed more significant than the target vehicle's speed ($v_j > v_i$), the target vehicle remains free-driving. If the preceding vehicle's speed is less than or equal to the target vehicle's speed ($v_j \le v_i$), the target vehicle will transition to the car-following state. Suppose the resultant potential field force between the target vehicle and the preceding vehicle exceeds the emergency braking threshold ($F_{ap} > F_{eb}$), with the preceding vehicle's speed more significant than the target vehicle's speed ($v_j > v_i$). In that case, the target vehicle maintains the car-following state. If the preceding vehicle's speed is less than or equal to the target vehicle's speed ($v_j \le v_i$), the target vehicle will transition to the emergency braking state. These longitudinal decision rules for the vehicle are expressed in an "IF-THEN" format, as shown in Table 3.

Table 3 Longitudinal state transition rules

Serial number	State transition rule
1	If $F_{ap} < F_{cf}$, $k_l = k_r = 0$ then State transition = 0
2	If $F_{cf} \le F_{ap} \le F_{eb}$, $k_l = k_r = 0$, and $v_j > v_i$ then State transition = 0; If $F_{cf} \le F_{ap} \le F_{eb}$, $k_l = k_r = 0$, and $v_j \le v_i$ then State transition = 1
3	If $F_{ap} > F_{eb}$, $k_l = k_r = 0$, and $v_j > v_i$ then State transition = 1; If $F_{ap} > F_{eb}$, $k_l = k_r = 0$, and $v_j \le v_i$ then State transition = 2

4.3 Formulation of lateral state transition rules

The resultant of lateral virtual potential field forces for AVs is expressed as Eq. (19):

$$F_{hc} = F_h + F_c = A\left(\cos\frac{2\pi y}{D_b} + 1\right) + \begin{bmatrix} k_l & 0 \\ 0 & k_r \end{bmatrix} \begin{bmatrix} (y - y_0)^a/\Delta y \\ -(y - y_0)^a/\Delta y \end{bmatrix} \tag{19}$$

Based on Eq. (19), the lateral decision transition rules can be formulated as follows: The transition of lateral decision behaviors primarily relies on the lateral decision coefficients. When $k_l = k_r = 0$, $F_{hc} = F_h$, indicating that the vehicle maintains a straight trajectory. When $k_l = 1$ and $k_r = 0$, $F_{hc} > F_h$. If the preceding vehicle's speed on the target lane is higher than the target vehicle's speed (i.e., $v_{oj} > v_i$), then the vehicle executes a left lane change. However, if the preceding vehicle's speed is lower than the target vehicle (i.e., $v_{oj} < v_i$), the vehicle continues straight driving. When $k_l = 0$ and $k_r = 1$, $F_{hc} < F_h$. If the preceding vehicle's speed on the target lane is higher than the target vehicle's speed (i.e., $v_{oj} > v_i$), then the vehicle performs a right lane change. If the preceding vehicle's speed is lower than the target vehicle (i.e., $v_{oj} < v_i$), the vehicle continues straight driving. These lateral decision rules are expressed as "If–Then" statements and presented in Table 4.

4.4 Establishment of decision-making model

Creating the decision model for an autonomous vehicle under emergency conditions requires distinct state transition rules as decision criteria. The autonomous vehicle determines its state in

Table 4 Lateral state transition rules

Serial number	State transition rule
1	If $k_l = k_r = 0$ then State transition = 0 or 1 or 2
2	If $k_l = 1, k_r = 0$, and $v_{oj} \leq v_i$ then State transition = 0 or 1 or 2; If $k_l = 1, k_r = 0$, and $v_{oj} > v_i$ then State transition = 3
3	If $k_l = 0, k_r = 1$, and $v_{oj} \leq v_i$ then State transition = 0 or 1 or 2; If $k_l = 0, k_r = 1$, and $v_{oj} > v_i$ then State transition = 3

an emergency scenario by processing surrounding environmental data. It employs a lateral lane-changing intent recognition model to ascertain whether it should continue longitudinally or initiate a lane change in the subsequent moment. Subsequently, decision rules governing the vehicle's driving behavior during emergency conditions are formulated based on the magnitudes of inter-vehicle potential field forces and the relative speeds between the subject vehicle and its preceding vehicle. The hierarchical state machine's structure for the established state transition rules is depicted in Fig. 7.

5 Simulation experiment

5.1 Establishment of integrated simulation model

Based on the actual road conditions of intelligent vehicles and the motion information of surrounding vehicles, an integrated simulation model is established, as illustrated in Fig. 8. The target vehicle and surrounding vehicle models are developed in the Carsim software, and the combined simulation model framework of the vehicle's potential field force model and the state machine decision model is constructed using Simulink.

The established joint simulation model, depicted in Fig. 8, primarily comprises three parts: the vehicle model, the vehicle's potential field force model, and the behavioral decision model.

5.1.1 *Vehicle model*

The signal input for the vehicle behavior decision model comes from the vehicle model. In this study, Carsim is utilized to establish the driving scenario of the autonomous vehicle. The output signals from the model include the position information of the target vehicle, the position information of surrounding vehicles, and the speeds of both the target vehicle and surrounding vehicles. The vehicle model can also accept input signals from external models, including wheel steering angles, accelerations, and other information, forming a closed-loop system with the output signals.

5.1.2 *Potential field force model*

The potential field force model can effectively plan vehicle motion information, thereby ensuring smoother movement of the

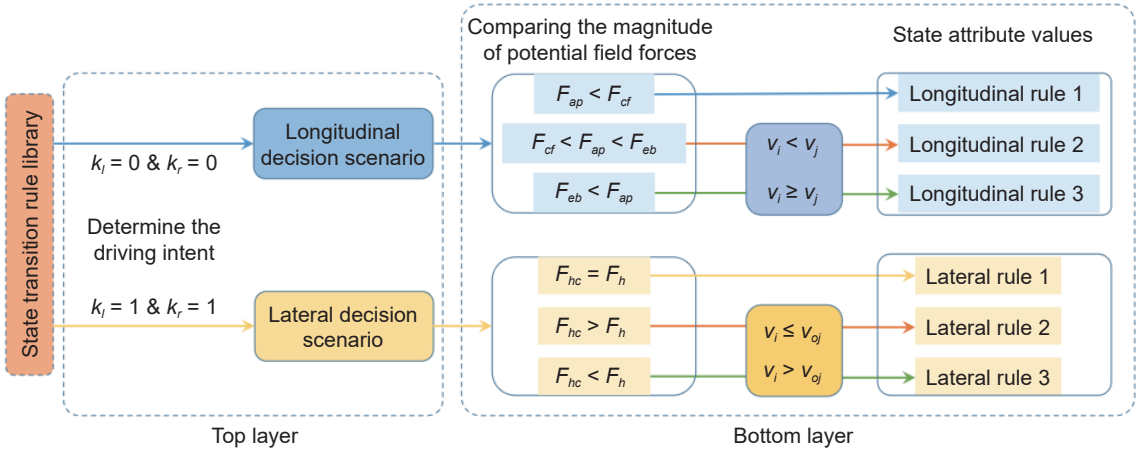

Fig. 7 Structure of the state transition rule repository.

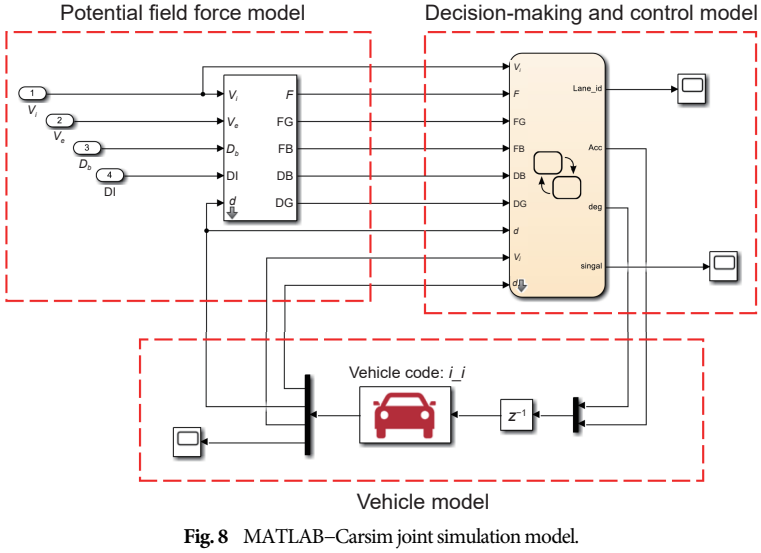

Fig. 8 MATLAB–Carsim joint simulation model.

autonomous vehicle. As a crucial decision indicator for the decision module, it can accurately assess the current motion state of the vehicle and provide data support for driving behavior decisions. This study's potential field force model uses the displacements between the target vehicle and surrounding vehicles as inputs. Real-time potential field forces are calculated using internal sub-modules, and the output includes the potential field force magnitudes for following and braking scenarios of the target vehicle. The potential field force output information serves as input for the decision model.

5.1.3 *Decision and control model*

The vehicle control module primarily executes signal output from the decision model, triggering different control methods within the control model based on different signals. This module encompasses two key functionalities: speed control and steering control. Following the established state transition rules and considering the specific driving environment and factors affecting vehicle driving behavior, the control module determines whether the vehicle should maintain its current lane or change lanes. When the target vehicle engages in longitudinal motion, activation of the longitudinal driving behavior rule library occurs, subsequently producing vehicle decision signals. The control module adjusts the vehicle's braking force and throttle accordingly. When the target vehicle is about to change lanes, the control module adjusts the vehicle's steering.

5.2 Simulation results

To validate the correctness of the model, regular driving vehicle information is set up for validation using the joint simulation model. Table 5 lists the critical parameters of the potential field force model and the initial positions and velocities of both the ego vehicle and surrounding vehicles during the vehicle simulation process. The variation in speeds of surrounding vehicles is set as illustrated in Fig. 9.

By incorporating the vehicle above and parameter model information into the joint simulation model, the variation curves of the potential field force's attraction and repulsive are obtained, as depicted in Fig. 10. By the rules governing the change in the resultant force of vehicle potential fields within the roads' coordinate system, thresholds are formulated for transitioning between different driving behaviors of the AVs. This ensures the issuance of accurate decision commands to the lower-level vehicle controller during the vehicle's progression, facilitating the realization of autonomous driving. The simulated decision output results are illustrated in Fig. 11, where lateral state transition decisions of the vehicle are produced during the time intervals of 30.0–30.4 s and 45–49 s, leading the vehicle to execute left and right lane-changing maneuvers, respectively. The corresponding potential field force variation curves indicate that the potential field force is null during lane-changing. Following the completion of the lane-changing, the decision model recalculates the vehicle's potential field force value. The vehicle maintains a longitudinal driving state throughout the other simulation periods, and the lane-change intent recognition model determines the satisfaction of lane-changing requirements.

Fig. 12 shows that during the initial 6.5 s of the simulation, the vehicle maintains its initial state of motion while experiencing virtual attractive force. This attractive force diminishes as the distance increases. As depicted in Fig. 13, the relative distance variation curve indicates that when the distance to the preceding vehicle reaches the vehicle's follow distance threshold, which is 60.5 m in this instance, the surrounding vehicle information is evaluated by the lane-change intent recognition model ($k = 0$), which determines that the lane-changing conditions are not met. Consequently, the vehicle continues to travel at 60 km/h while maintaining the following mode. At 24.5 s, with the target vehicle's distance from the preceding vehicle reduced to 33.4 m, the lane-change model recognizes that the vehicle still needs to remain longitudinal. This prompts the vehicle to enter an emergency braking state, where a substantial braking force is applied to reduce the speed to 54 km/h, ensuring a safe following distance between the two vehicles. At 30.0 s, the lane-change intent recognition model ($k = 1$) evaluates the neighboring lane's vehicle information, determining that the conditions for changing lanes into the adjacent lane are met. Consequently, the target vehicle initiates an acceleration-based lane-changing maneuver.

Table 5 Main parameters of joint simulation experiments

Simulation parameter	Value
Position gradient of attractive force, α	6
Position gradient of repulsive force, n	0.5
Vehicle lane change time (s)	4
Initial velocity of the target vehicle (km/h)	75
Initial position of the target vehicle (m)	(−2, 80)
Initial position of vehicle on adjacent lane (m)	(2, 50)
Initial position of the vehicle ahead (m)	(−2, 100)

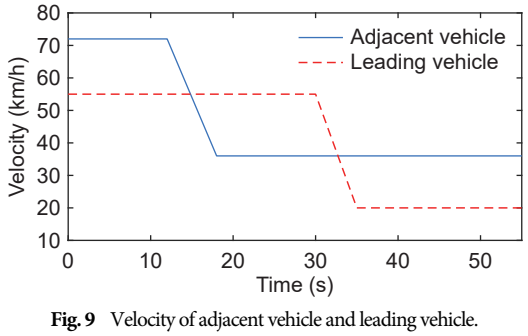

Fig. 9 Velocity of adjacent vehicle and leading vehicle.

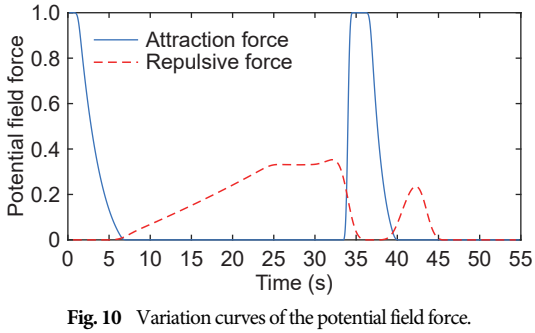

Fig. 10 Variation curves of the potential field force.

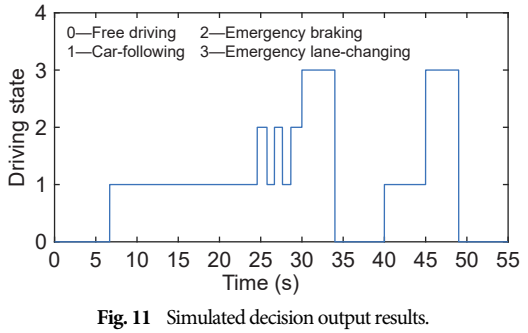

Fig. 11 Simulated decision output results.

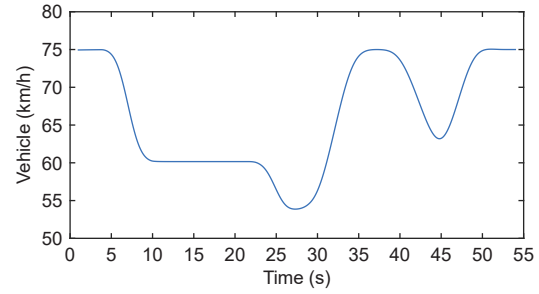

Fig. 12 Velocity variation curve.

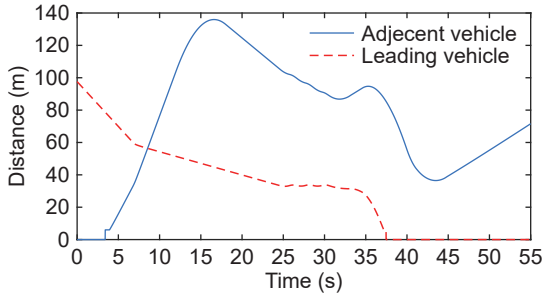

Fig. 13 Distance variation of surrounding vehicles.

When the target vehicle transitions to the overtaking lane (34.0–45.0 s), the potential field force model recalculates the values of the forces exerted by the vehicles ahead in the current lane. Upon completion of the lane change, the distance between the target vehicle and the leading vehicle in the current lane becomes more significant than the following distance threshold. At this point, the vehicle continues to experience the vehicle attractive force state. The target vehicle resumes the following behavior as the distance reaches the threshold. At 45.0 s, the lane-change intent recognition model ($k = -1$) determines that the neighboring lane's vehicle information meets the lane-changing conditions. Consequently, the target vehicle returns to its original lane and travels at the desired speed.

The analysis of the aforementioned combined simulation results concludes that by providing the target vehicle with a desired speed, the developed decision model in this study accurately generates driving behaviors of the vehicle at different time intervals. These behaviors serve as signals to trigger the control module, enabling the vehicle to perform motion planning accurately.

6 Conclusions

This study initially introduces the fundamental principles and framework of FSMs, analyzing the elements within the state machine of AVs. A hierarchical vehicle state machine decision model is proposed. Based on the vehicle potential field model, mathematical models for determining the transition thresholds of lateral and longitudinal vehicle states are established, leading to the formulation of transition rules between different states of AVs. Subsequently, a vehicle hierarchical state machine model and a vehicle control model are constructed using Simulink. Finally, a combined simulation model is developed with Carsim–MATLAB platform to verify the feasibility of the proposed vehicle driving behavior decision strategy.

Replication and data sharing

The MATLAB program code within this research can be made accessible upon request via email to the corresponding author.

Declaration of competing interest

The authors have no competing interests to declare that are relevant to the content of this article.

Acknowledgements

This work was supported by the National Natural Science Foundation of China (Grant No. 52102454), and the Postdoctoral Science Foundation of China (Grant No. 2021M700169); in part by the Natural Science Foundation of Chongqing (Grant No. cstc2021jcyj-msxmX0395), the Special Funding for Postdoctoral Research Projects in Chongqing (Grant No. 2021XM3069), the Youth Project of Science and Technology Research Program of Chongqing Education Commission of China (Grant Nos. KJQN202001302 and KJQN202203909), the Natural Science Foundation of Yongchuan District (Grant No. 2023yc-jckx20089), and the Opening Project of Intelligent Policing Key Laboratory of Sichuan Province (Grant No. ZNJW2023KFQN002).

References

Guo, N., Zhang, X., Zou, Y., 2022. Real-time predictive control of path following to stabilize autonomous electric vehicles under extreme drive conditions. Automot Innov, 5, 453–470.

He, Y., Liu, Y., Yang, L., Qu, X. 2023. Deep adaptive control: Deep reinforcement learning-based adaptive vehicle trajectory control algorithms for different risk levels. IEEE Trans Intell Veh, 9, 1654–1666.

Jaswanth, M., Narayana, N. K. L., Rahul, S., Supriya, M., 2022. Autonomous Car Controller using Behaviour Planning based on Finite State Machine. In: 2022 6th International Conference on Trends in Electronics and Informatics (ICOEI), 296–302.

Li, H., Liu, W., Yang, C., Wang, W., Qie, T., Xiang, C., 2022. An optimization-based path planning approach for autonomous vehicles using the DynEFWA-artificial potential field. IEEE Trans Intell Veh, 7, 263–272.

Liang, Y., Li, Y., Yu, Y., Zhang, Z., Zheng, L., Ren, Y., 2021. Path-following control of autonomous vehicles considering coupling effects and multi-source system uncertainties. Automot Innov, 4, 284–300.

Liu, Y., Lyu, C., Zhang, Y., Liu, Z., Yu, W., Qu, X., 2021. DeepTSP: Deep traffic state prediction model based on large-scale empirical data. Commun Transport Res, 1, 100012.

Liu, Y., Wu, F., Liu, Z., Wang, K., Wang, F., Qu, X., 2023a. Can language models be used for real-world urban-delivery route optimization? Innovation, 4, 100520.

Liu, Z., Li, Y., Wu, Y., 2023b. Multiple UAV formations delivery task planning based on a distributed adaptive algorithm. J Frankl Inst, 360, 3047–3076.

Ma, H., An, B., Li, L., Zhou, Z., Qu, X., Ran, B., 2023a. Anisotropy safety potential field model under intelligent and connected vehicle environment and its application in car-following modeling. J Int Con Veh, 6, 79–90.

Ma, Y., Dong, F., Yin, B., Lou, Y., 2023b. Real-time risk assessment model for multi-vehicle interaction of connected and autonomous vehicles in weaving area based on risk potential field. Phys A Stat Mech Appl, 620, 128725.

Nguyen, H. D., Choi, M., Han, K., 2023. Risk-informed decision-making and control strategies for autonomous vehicles in emergency situations. Accid Anal Prev, 193, 107305.

Palatti, J., Aksjonov, A., Alcan, G., Kyrki, V., 2021. Planning for safe abortable overtaking maneuvers in autonomous driving. In: 2021 IEEE International Intelligent Transportation Systems Conference (ITSC), 508–514.

Rasekhipour, Y., Khajepour, A., Chen, S. K., Litkouhi, B., 2017. A potential field-based model predictive path-planning controller for autonomous road vehicles. IEEE Trans Intell Transport Syst, 18, 1255–1267.

Wang, W., Qie, T., Yang, C., Liu, W., Xiang, C., Huang, K., 2022a. An

intelligent lane-changing behavior prediction and decision-making strategy for an autonomous vehicle. IEEE Trans Ind Electron, 69, 2927–2937.

Wang, X., Qi, X., Wang, P., Yang, J., 2021. Decision making framework for autonomous vehicles driving behavior in complex scenarios via hierarchical state machine. Auton Intell Syst, 1, 10.

Wang, Y., Cao, X., Ma, X., 2022b. Evaluation of automatic lane-change model based on vehicle cluster generalized dynamic system. Automot Innov, 5, 91–104.

Xie, S., Hu, J., Bhowmick, P., Ding, Z., Arvin, F., 2022. Distributed motion planning for safe autonomous vehicle overtaking via artificial potential field. IEEE Trans Intell Transport Syst, 23, 21531–21547.

Zheng, X., Huang, B., Ni, D., Xu, Q., 2018. A novel intelligent vehicle risk assessment method combined with multi-sensor fusion in dense traffic environment. J Intell Connect Veh, 1, 1–14.

Xunjia Zheng received the Ph.D. degree in mechanical engineering from Tsinghua University, Beijing, in 2020. He is currently an associate professor with the School of Intelligent Manufacturing Engineering, Chongqing University of Arts and Sciences, Chongqing. His current research interests include vehicle active safety systems, mobile robots, and intelligent vehicles.

Huilan Li received the B.S. and M.S. degrees in the School of Mechatronics and Vehicle Engineering from Chongqing Jiaotong University, Chongqing, in 2016 and 2019, respectively. She is currently pursuing the Ph.D. degree in the School of Traffic and Transportation at Chongqing Jiaotong University, and also is currently an assistant professor at the Department of Information and Intelligence Engineering Chongqing City Vocational College, Chongqing. Her current research interests include connected and automated vehicles, risk assessment, decision-making, situational awareness, and prediction.

Qiang Zhang received the B.S. and M.S. degrees in automation from Harbin Engineering University and vehicle engineering from Tsinghua University, in 2006 and 2015, respectively. He is currently a professor of engineering, serves as the Vice General Manager of the Information Intelligence Division at China Automotive Engineering Research Institute Co., Ltd. (CAERI) and concurrently holds the position of General Manager at CAERI Intelligent Connected Vehicle Technology Co., Ltd. Additionally, he serves as the Deputy Director of the National Key Laboratory of Intelligent Vehicles. His current research interests encompass intelligent driving technology and evaluation techniques for intelligent vehicle testing.

Yonggang Liu received the B.S. and Ph.D. degrees in automotive engineering from Chongqing University, in 2004 and 2010, respectively, and the joint Ph.D. degree from the University of Michigan–Dearborn, MI, USA, in 2009. He is currently a professor, a Doctoral Supervisor, and the dean assistant with the School of Automotive Engineering, Chongqing University. His research interests include optimization and control of intelligent electric vehicles (EV/HEV) power systems, and integrated control of vehicle automatic transmissions.

Xing Chen received the Ph.D. degree in mechanical engineering from Beijing Institute of Technology in 2015. He is currently a professor with the School of Intelligent Manufacturing Engineering, Chongqing University of Arts and Sciences, Chongqing. His research interests include autonomous driving, and nonlinear vehicle dynamics.

Hui Liu received the Ph.D. degree in mechanical engineering from Chongqing University in 2017. He is currently an associate professor with the School of Intelligent Manufacturing Engineering, Chongqing University of Arts and Sciences, Chongqing. His research interests include autonomous driving and vehicle platoon control.

Tianhong Luo received the B.S., M.S., and Ph.D. degrees in mechanical engineering from Chongqing University in 1998, 2002, and 2005, respectively. He is currently a professor with the School of Intelligent Manufacturing Engineering, Chongqing University of Arts and Sciences, Chongqing. His research interests include mobile robots, industrial robots, and service robots.

Jianjie Gao received the B.S. degree in the School of Transportation and Vehicle Engineering with Shandong University of Technology and M.S. degree in the School of Mechatronics and Vehicle Engineering from Chongqing Jiaotong University, in 2008 and 2010, respectively. He is currently an associate professor at the Intelligent Policing Key Laboratory of Sichuan Province. His current research interests include automated vehicles and transportation safety.

Lihong Xia received the B.S. and Ph.D. degrees in vehicle engineering from Chongqing University, Chongqing, China, in 2009 and 2019, respectively. Since 2019, she has been a lecturer with the Department of Vehicle Engineering, University of Chongqing Technology and Business. Her research interests include Intelligent and Connected Vehicles, with an emphasis on driving behavior analysis and prediction, driving safety assessment, driving decision making, and test and evaluation